- Technical Paper -

CONTRIBUTION OF SURROUNDING RC FRAME AND MASONRY WALL IN LATERAL RESISTANCE OF MASONRY INFILLED RC FRAME

Debasish SEN[*1], Hamood ALWASHALI[*1], Kiwoong JIN[*2] and Masaki MAEDA[*3]

ABSTRACT

Masonry infilled RC buildings act as composite structure and the contribution of each element is not clear under seismic loading. Therefore, the contribution of surrounding RC frame and infilled masonry has been estimated from experimental investigation of five half-scaled masonry infilled RC frames. In addition, the ultimate drift, after which masonry degrades rapidly, has also been evaluated. The observed results indicate that relative shear strength of RC frame to masonry dictates the contribution of RC frame and, the conservative ultimate drift of infilled masonry can be considered at 0.6% drift angle.

Keywords: RC frame, Masonry wall, Seismic evaluation, Contribution factor by infill and boundary frame, Drift limit.

1. INTRODUCTION

Masonry infilled RC frame is a widely used structural system in developing countries due to availability of materials. Many masonry infilled RC buildings are located in earthquake prone areas which are required to be evaluated for seismic vulnerability. Generally, contribution of masonry wall as a structural element is not considered in building design codes, since the beneficial or detrimental effects of masonry wall on the overall structural behavior have not been concretely established yet. However, recent earthquake damages e.g. Mexico earthquake (2016), Nepal earthquake (2015) showed the strong evidence about the interaction of non-structural elements, e.g. masonry walls with the seismic damage of buildings [1]. Hence, for the seismic evaluation of existing buildings as well as for economic design of new buildings, the contribution of masonry wall should be considered. Previous experimental endeavor on masonry infilled RC frame [1] showed that, at the initial stage of load resistance, the masonry wall and surrounding RC frame work as a combined unit. However, due to the formation of gap between surrounding frame and infill masonry, the load is resisted by diagonal strut, formed in the wall, and the surrounding frame. Consequently, hinges are formed in surrounding frame, which expedite deformation of the infill masonry and results in subsequent deterioration of load carrying capacity of the masonry wall. In addition, the contribution of masonry and surrounding frame might not be equal at all drift stages, since the combined behavior of masonry infilled RC frame is complicated. Therefore, endeavor is necessary to find the contributions of each constituent part (i.e. infill masonry and surrounding RC frame) separately. Especially for seismic evaluation, it is necessary to find out the ultimate drift level (R_1) where the masonry infill reaches its maximum strength, and the proportion (V_1) of load carried by RC frame, as shown in Fig. 1. Hereafter, contribution of RC frame at any drift will be addressed as contribution factor (α), which is the ratio of contribution of RC frame (V_1) at that drift to its ultimate capacity of the frame ($V_{fr,ult}$).

The objective of this study is two folds: first, to find out the contribution of the RC frame and masonry wall separately in the overall frame under cyclic lateral loadings, experimentally and analytically; and secondly, to find out the ultimate drift level of infill masonry and the contribution of RC frame at that drift. It should be also noted that the in-plane behavior or collapse are only focused in this study, as a first step.

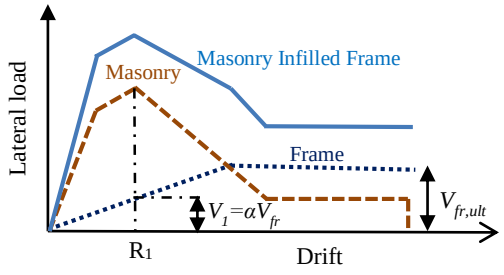

Fig. 1 Typical load-drift curve of infilled frame

2. EXPERIMENTAL PROGRAM

2.1 Specimen Details

Five one bay single story masonry infilled RC frames have been designed. RC frames have been designed using a strong beam-weak column concept, except one specimen. RC columns have been designed as flexural columns to avoid shear failure of the column under lateral load. For all specimens, masonry wall thickness is 100mm. The infill panel have been constructed using 60 x 100 x 210mm solid bricks. Mortar head and bed joint thicknesses are 10mm. The main variables of specimens are relative shear strength of RC

*1 Graduate School of Engineering, Tohoku University, JCI Student Member
*2 Assistant Prof., Dept. of Architecture and Building Science, Tohoku University, Dr.E., JCI Member
*3 Professor, Dept. of Architecture and Building Science, Tohoku University, Dr.E., JCI Member

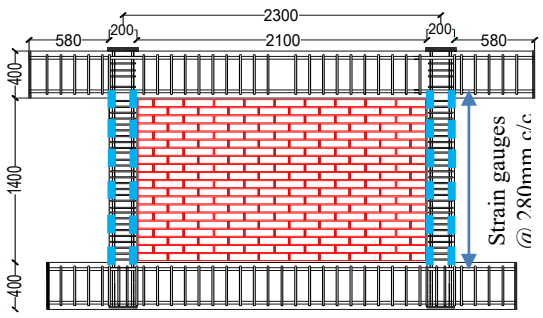

Fig. 2 Typical geometry of specimens

frame to masonry wall, joint mortar strength of masonry wall and relative moment capacity of beam. Typical geometry of the specimen is shown in Fig. 2, where all dimensions are in mm. Specimens namely strong frame (SF) and weak frame (WF) represent the specimens with varying relative shear strength of RC column to masonry infill. Bounding RC frames are identical in strong mortar (SM) and weak mortar (WM) specimens, however, the difference is in the strength of joint mortar. The major difference between specimen WF and SM is in column reinforcements which increase the moment capacity, as shown in Table 1, along with the lateral capacity about 40%. Lastly, weak beam (WB) specimen represents a strong column-weak beam type RC frame infilled with masonry. It is to be noted that mortar strengths of masonry joints of all specimens are intended to be the same except for the weak mortar (WM) specimen, where strength is intentionally reduced. Summary of specimen characteristics are shown in Table 1. More details characteristics are referred to author's previous work [1].

2.2 Materials

(1) Concrete and reinforcement

The mean compressive strength, Young's modulus and split tensile strength of three concrete cylinders are stated in Table 2. Concrete cylinders were built at the same time with frame casting. Compressive and split tensile strength tests conformed to JIS A 1108 (2010) and JIS A 1113 (2010) standards [2], respectively. The yield and ultimate tensile strength of column reinforcements are about 380MPa and 560MPa respectively.

(2) Masonry

Masonry prism and mortar cylinder samples were made simultaneously with the infill panel. Masonry prisms were tested for compressive strength according to ASTM C 1314 (2011) [3], whereas compressive strength tests of mortar cylinder conformed to JIS A 1108 (2010) [2]. All test results of compression test on masonry prisms and mortar cylinders are shown in Table 3.

2.3 Instrumentation and Loading

Strain gauges, shown in Fig. 2 have been attached on both tension and compression reinforcements of columns, with a spacing of 280mm to get the internal strain of reinforcements. The schematic diagram of loading system is shown in Fig. 3. The vertical load has been applied on RC columns by two vertical hydraulic jacks and maintained 200 KN on each column.

Table 1 Details of specimen

Spec-imen	RC column (mm)	Upper beam (mm)	Steel in column	Column Moment capacity (KN-m)
SF	300x300	600x400	8-D16	99.1
WF	200x200	600x400	4-D10	25.4
SM	200x200	600x400	4-D16	40.4
WM	200x200	600x400	4-D16	40.4
WB	200x200	200x250	4-D16	40.4

Table 2 Concrete properties

Specimen	f_y (MPa)	E (MPa)	f_t (MPa)
SF	28.3	23000	2.4
WF	24.2	23000	2.1
SM	25.5	24000	2.0
WM	25.8	23000	2.0
WB	23.6	24000	1.9

f_y= Compressive strength, E= Elastic modulus and f_t= Split tensile strength

Table 3 Properties of masonry

Specimen	Masonry Prism			Mortar
	f_y (MPa)	E (MPa)	ε_{peak} (μ)	f_y (MPa)
SF	18.6	8140	3900	29.2
WF	17.3	7840	3700	20.2
SM	19.5	10230	3600	27.7
WM	13.3	5470	5900	4.80
WB	19.5	10230	3600	27.7

f_y= Compressive strength, E= Elastic modulus and ε_{peak}= Strain at peak strength

Two pantographs, attached with the vertical jacks, restricted any torsional and out-of-plane displacement. Two horizontal jacks, applying together for an incremental cyclic loading, have been attached at the beam level and controlled by a drift angle. Drift angle (R), defined as the percentage of lateral story deformation to the story height at the middle depth of the beam, is measured using transducer displacements. The lateral loading program consisted of 2 cycles for each peak drift angle of 0.05, 0.1, 0.2, 0.4, 0.6, 0.8, 1, 1.5 and 2%.

3. EXPERIMENTAL RESULTS

In this section, the overall behavior and hinge formation mechanism of windward column (i.e. in tension) of tested specimens are presented, which is related to the objective of this study. The hysteresis curves of lateral load vs. drift angle of all specimens under cyclic loadings are shown in Fig. 4. Strong frame (SF) specimen showed higher lateral load capacity, which is about 2 times of those in weak frame (WF) specimen. In the strong frame (SF) specimen, long reinforcements yielded at the upper and bottom critical section of tension column, which is similar to a bare frame. Whereas, in weak frame (WF) specimen, the longitudinal reinforcement of tensile column yielded at the upper critical section and above its mid height, forming failure mechanism similar to a short column.

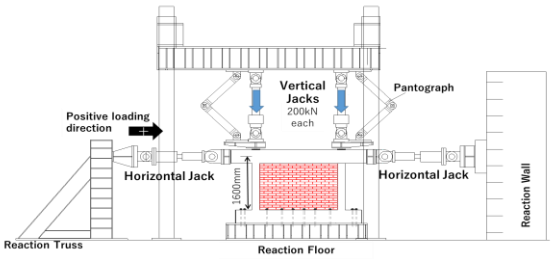

Fig. 3 Schematic diagram of loading system

Strong mortar (SM) specimen showed almost same lateral load capacity and deformation at maximum strength as weak mortar (WM) specimen. In the strong mortar (SM) specimen, the long reinforcements in the tensile column yielded at the upper critical section and almost at the mid height. The horizontal crack formation in the masonry infill might be attributed for this mechanism. Whereas, in the weak mortar (WM) specimen tensile column reinforcements yielded at the upper and bottom section like a bare frame. Weak beam (WB) specimen showed almost 10% reduction in maximum lateral strength compared with the strong mortar (SM) specimen (which has same structural configuration with weak beam (WB) specimen except the beam size). The deformation capacities are almost the same (0.8% drift) at the peak load with strong mortar (SM) specimen. In tensile column, reinforcements yielded at just below the mid height and at the upper beam. In the all specimens, hinges have been formed at the top and near the bottom of compression column.

It is evident from the experimental results that the behaviour of masonry infilled RC frames has been influenced by relative strength of column, mortar strength and beam capacity. In addition, it is obvious from hysteresis curves of all specimens that the behavior of masonry infilled RC frame is almost symmetric under cyclic loadings. The differences in maximum load carried by infilled frame between positive and negative cycle is not high, except weak frame (WF) specimen. Therefore, positive cycle has been representatively chosen for the further analysis of getting contribution of RC frame and masonry wall separately, which will be discussed in the following sections.

4. INDIVIDUAL CONTRIBUTION OF BOUNDING RC FRAME AND MASONRY WALL

In this study, the contribution of bounding RC frame at a certain drift angle has been calculated from the experimental data using two methods - 1) Analysis of the strains of column reinforcements and, 2) Tri-linear analytical model of column. This is followed by the determination of masonry infill's contribution at that drift by using Eq. 1. The theoretical analysis process of estimating surrounding frame's contribution is presented in the following section.

$$v_{mas} = v_{exp} - v_{fr} \quad (1)$$

where, v_{mas} :load carried by masonry wall
v_{exp} :load carried by overall frame
v_{fr} :load carried by surrounding RC frame

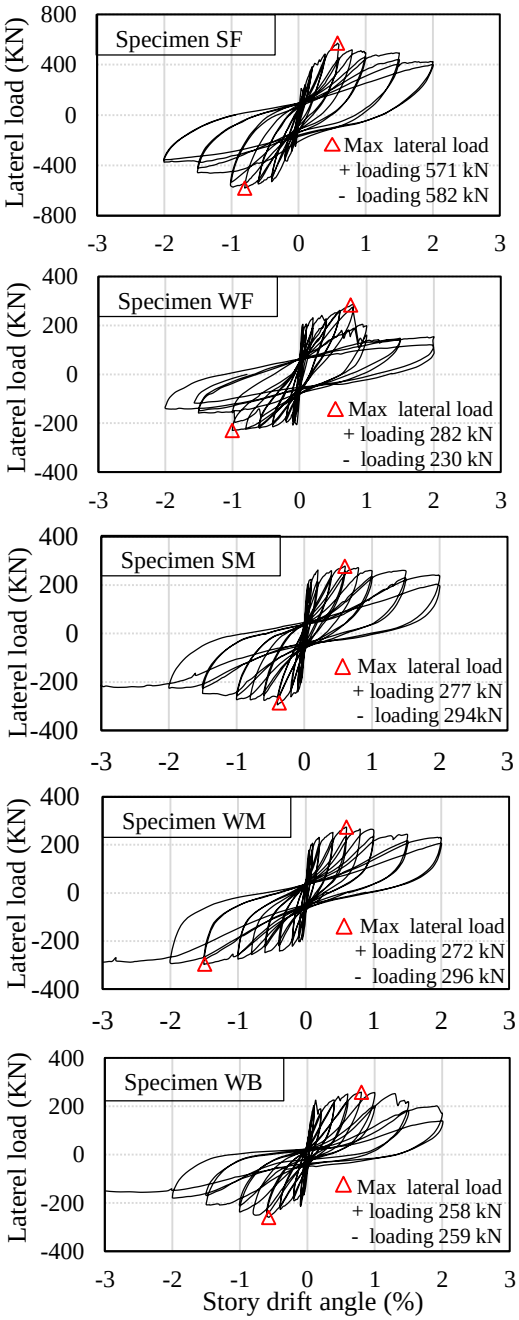

Fig. 4 Hysteresis curve of specimens

4.1 Analysis of Strains of Column Reinforcements

The recorded strain values have been initially analyzed to get the bending moment diagram and curvature distribution along the column height at a certain drift angle. The curvature distribution has been used to get the effective height of columns. Subsequently, lateral load carried by bounding RC column has been determined from the bending moment using Eq. 2. It is to be noted that hinge locations of masonry infilled frame might not be at the top and bottom of column, as in bare frame, therefore effective height of two actual hinges are computed to be used in frame's lateral load calculation.

$$v_{fr} = \frac{M_{c,top} + M_{c,bottom}}{h_o} \quad (2)$$

where, v_{fr} : shear resisted by surrounding frame
$M_{c,top}$: top moment of column (or beam)

$M_{c,bottom}$: moment at the bottom of column
h_o : effective column height

(1) Estimation of bending moment distribution

The strain values in tension and compression side reinforcements of columns have been employed to get the strain profile on column sections using plane section assumption. Based on the concrete strains, Todeschini continuous curve [4] of concrete stress distribution has been used to estimate the average compressive stress on concrete using Eqs. 3 and 4. Schematic diagram of stress distribution on the column section is outlined in Fig. 5.

$$\bar{f}_c = \frac{\ln[1+(\varepsilon_{max}/\varepsilon_o)^2]}{(\varepsilon_{max}/\varepsilon_o)} \cdot f_c \quad (3)$$

$$a = \left[1 - \frac{2(x_1 - \tan^{-1} x_1)}{x_1^2 \beta_1}\right] .c \quad (4)$$

where, $\bar{f}_c$: average stress on concrete
f_c : stress at the outer face of column
ε_{max} : strain at the outer face of column
ε_o : strain at maximum stress

Meanwhile, the forces acting on steel location has been obtained from the strain values of reinforcement considering a bilinear model. This is followed by the estimation of bending moment exerted by the lateral loads at the places where strain gauges have been attached on the reinforcements, using internal forces of column sections. After getting moment at each section, bending moment diagram of entire column at a certain drift angle have been estimated.

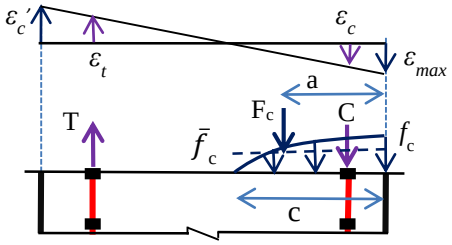

Fig. 5 Schematic diagram of stress-strain distribution on column section

(2) Estimation of column's effective height

The effective height has been estimated from the distribution of curvature along with moment distribution along the column height. The curvature (φ) at a certain height has been evaluated using strains recorded by two strain gauges affixed on the tensile and compression longitudinal bars at that level using the Eq. 5.

$$\varphi = \frac{\varepsilon_t - \varepsilon_c}{l} \quad (5)$$

where, ε_t : strain of tensile reinforcement
ε_c : strain of compressive reinforcement
l : c/c distance of reinforcements

Moment and curvature distribution along with ultimate moment capacity, yield curvature of strong mortar (SM) specimen at 0.8% drift angle are presented in Fig. 6(a) and Fig. 6(b). Moment distribution and curvature distribution along column height show similar pattern, hence curvature distribution has been employed to determine the effective height of column. Yield curvature of column has been set as the criteria to find out the location of hinge formation. The yield curvature has been calculated using yield strain of column reinforcement [5]. Utilizing aforementioned criteria, the effective clear height of tension and compression column of strong mortar (SM) specimen has been estimated as 0.82m and 1.4m, respectively, which resembled with the experimental observation discussed earlier. Hence, for the other specimens, same procedure has been followed to evaluate effective height of column. It is to be noted that, in weak beam (WB) specimen, the hinge has been formed at upper beam and bottom of columns.

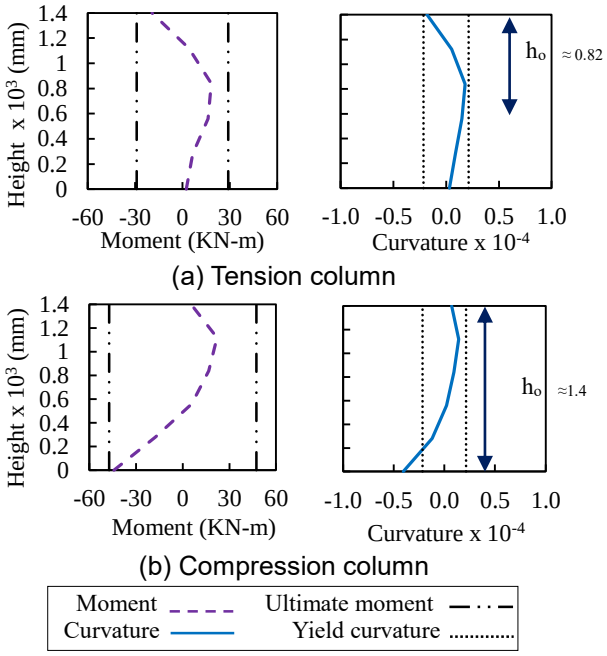

Fig. 6 Moment and curvature distribution of (a) tension and (b) compression column at 0.8% drift angle for strong mortar (SM) specimen

4.2 Using Tri-linear Analytical Model of Column

Tri-linear analytical model of columns proposed in AIJ 2010 [6], shown in Fig. 7(a), has been employed to find out the lateral load and drift angle relation of each column. Initial stiffness (K_c) and secant stiffness (K_e) of column has been determined using Eqs. 6. to 8. To determine the ultimate (M_u) and cracking (M_{cr}) moment capacity of RC columns with the effect of infill, axial forces (Q_B) exerted by the infill on column has been considered herein, along with externally imposed axial force (N). The change in axial force (Q_B), at cracking and ultimate state, has been estimated by solving equilibrium equations of surrounding RC frame using free body diagram shown in Fig. 7(b). It is to be noted that, hereafter left (windward) and right (leeward) side columns of the frame for the lateral loading shown in Fig. 7(b) will be termed as tension and compression column respectively.

$$K_c = \left(\frac{12EI_c}{h^3} \cdot \frac{12\rho+1}{12\rho+4}\right) \quad (6)$$

$$K_e = \alpha_y K_c \quad (7)$$

$$\alpha_y = (0.043 + 1.64nP_t + 0.043(a/d) + 0.33\eta_o)\left(\frac{d}{D}\right)^2 \quad (8)$$

where, ρ : beam to column sectional rigidity ratio
n : elastic modulus ratio of steel and concrete
P_t : percent of tensile reinforcement
a : shear span of column
d : effective depth of column
D : column depth

At ultimate and cracking states, lateral load (P) has been considered as the experimental maximum lateral load (P_{max}) and one-third of the maximum lateral load ($P_{max}/3$) for the overall frame. Moment capacities has been determined using Japanese standard [6]. Using the top and bottom moment of columns' and the effective height, lateral load resisted by RC column has been estimated using Eq. 2. After that the backbone curve of each column has been estimated using ultimate and cracking load with corresponding stiffness. Afterward, the backbone curves of two columns have been superimposed to get the backbone curve of RC frame.

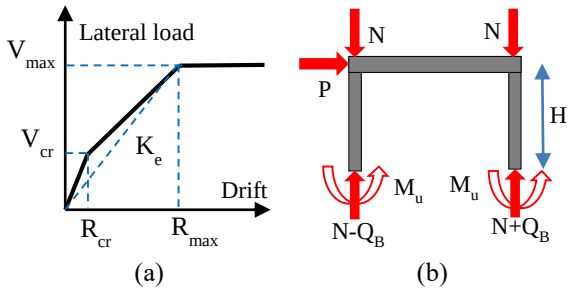

Fig. 7 (a) Tri-linear analytical model for RC column and (b) Free body diagram of surrounding frame

5. RESULTS AND DISCUSSION

The backbone curves of masonry infilled RC frame (obtained from experimental program), and separated contribution by bounding RC frame (both by strain values and analytical model) and masonry wall for all specimens are presented in Fig. 8. Strain gauge values have been used up to 1% drift, because reinforcements yielded around this drift, after that strain gauges might not give reliable results. Fig. 8 also includes the ultimate drift of infilled masonry suggested by Alwashali [1] and ASCE [7] based on the masonry prism strain at peak strength and the relative strength of frame to masonry, respectively.

From the observed behavior of masonry wall, it is evident that in all cases masonry starts to crack within a range of 0.1~ 0.2% drift. From Fig. 9 it is evident that, at 0.2% drift angle, contribution of RC frame is below 20%, except the infilled masonry with very strong frame (SF) or very weak frame (WF) where contribution is about 25%. After first cracking, masonry wall sustained the load up to a drift angle, after which it starts to degrade rapidly. This drift level varies with the frame strength, mortar strength and beam capacity. Masonry wall of strong frame (SF), strong mortar (SM) and weak mortar (WM) specimens have reached its maximum at

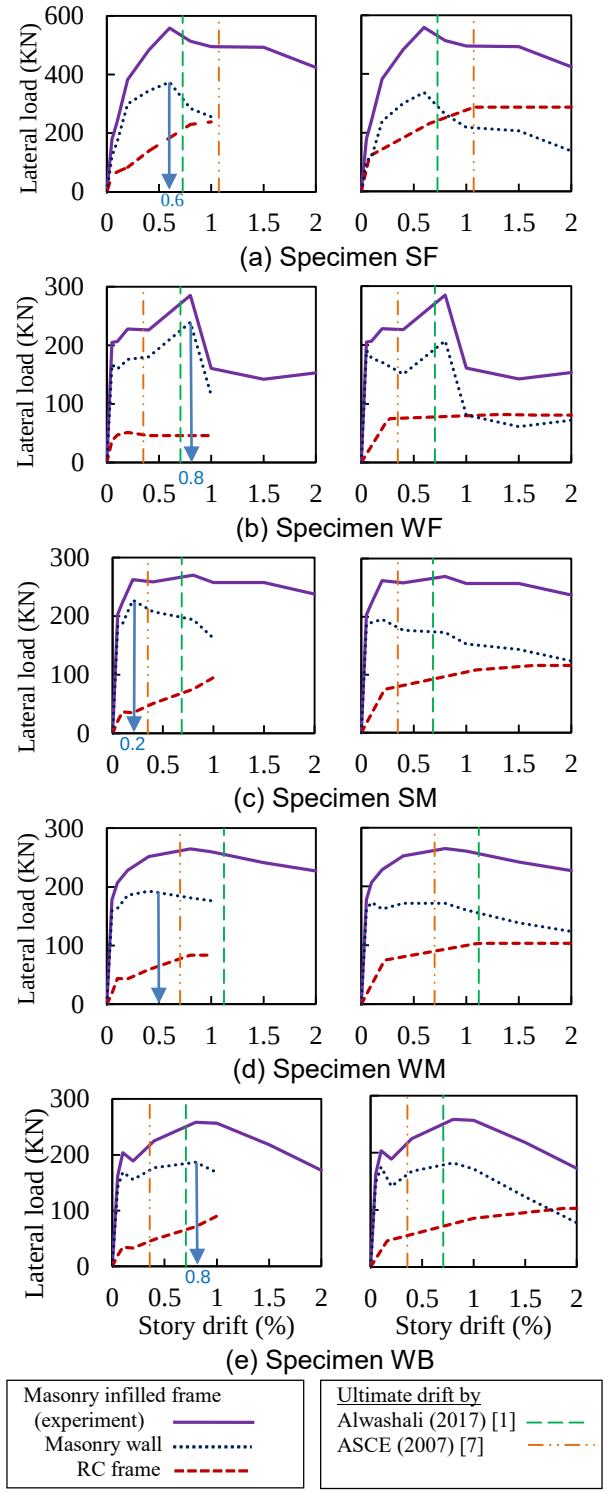

Fig. 8 Backbone curve of surrounding RC frame by strain gauge (left) and analytical model (right) along with masonry wall and masonry infilled frame

about 0.6% drift, whereas masonry in weak frame (WF) or weak beam (WB) specimens have reached its maximum at a drift greater than 0.6%. At maximum strength of masonry, the contribution of RC frame is about 35% for strong frame (SF) specimen, whereas those for strong mortar (SM) and weak mortar (WM) specimens are about 25%. For weak frame (WF) specimen, the contribution of RC frame is about 20%. From the calculated contribution of RC frame, it is

evident that the relative strength of RC frame to masonry plays an important role on the contribution of surrounding RC frame and most of the lateral load has been carried by the masonry wall until 0.6% drift angle. After that, at 0.8% drift, where overall masonry infilled frame reached its maximum, the contribution of RC frame increased, except for the weak frame (WF) specimen in which frame reached its capacity before 0.8% drift, which indicates that RC frame have not reached to ultimate yet, which is also evident in moment distribution in Fig. 6.

To be conservative, 0.6% drift level until which masonry takes most of the loads without massive crack, is considered to be the ultimate drift limit (R_1) for the infilled masonry. From Fig. 8, it is evident that the model suggested by Alwashali [1] showed good agreement to predict the ultimate drift of masonry than ASCE 2007 [7], which employs masonry prism strain at maximum strength. Hence, strain at maximum strength of masonry prism is closely related to the ductility of infilled frame.

Contribution factor (α) as a function of drift are shown in Fig. 10, where, contribution factor at a certain drift has been calculated, using Fig. 8, as the ratio of frame resistance at that drift to the ultimate resistance of the frame. To determine contribution factor at the peak strength of masonry, conservative ultimate drift level of masonry, discussed earlier, has been used because ultimate drift level varies specimen by specimen, as shown in Fig. 8. At the conservative ultimate drift level (R_1= 0.6%), the range of contribution factor of RC frame is found to be 0.65~0.85, without considering WF specimen which reached its maximum capacity prior to this drift.

It is evident from Fig. 8 that, the analytical model of frame somewhat overestimates the cracking strength of the frame, however it can predict the overall behavior which is similar to the experimental behavior. From Fig. 11, it is evident that, at 0.8% drift analytical model can predict the strength of surrounding RC frame precisely than that at the drift 0.2%. Therefore, the analytical model can be used to predict the behavior of surrounding frame, especially ultimate strength of surrounding frame with good accuracy.

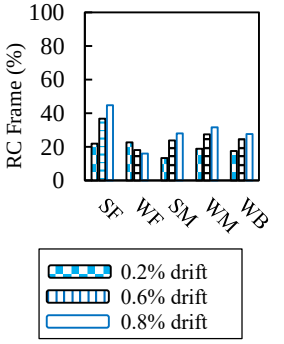

Fig. 9 Contribution of RC frame at different drifts

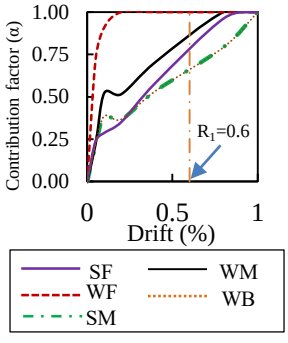

Fig. 10 Contribution factor of RC frame at different drifts

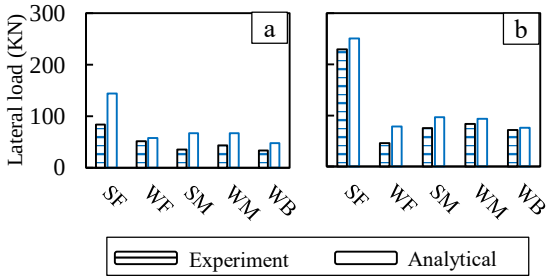

Fig. 11 Comparison of experimental and analytical load at (a) 0.2% and (b) 0.8 % drift angle

6. CONCLUSIONS

In this study, the strain data of column reinforcements and an analytical model have been employed to determine the contribution by the constituent parts of masonry infilled frame. Important findings are summarized as below.

(1) In this experiment masonry walls have started cracking within a range of 0.1~ 0.2% drift. Subsequently, masonry infills have reached its maximum strength at about 0.6% drift, after exceeding this drift level masonry infill have started to degrade rapidly and most of the lateral load has been carried by the masonry wall until this drift. This drift can be considered as the ultimate drift of infilled masonry, which depends on the strain at peak compressive strength of masonry prism.

(2) Relative strength of surrounding RC frame to masonry is the key parameter which has profound influences on the contribution of surrounding RC frame at different stages of drift.

(3) In this study the contribution factor of RC frame at ultimate drift of masonry has been found about 0.65~0.85, except masonry in very weak frame, which can be considered for seismic evaluation.

(4) Tri-linear lateral load model used in this study for the boundary frame, considering the axial load exerted by infill wall, overestimates first cracking load. However, it can predict fairly the ultimate strength at higher drift.

ACKNOWLEDGEMENT

This research is supported by SATREPS project lead by Prof. Nakano Yoshiaki, Tokyo University. Authors would like to acknowledge the cordial help of Mr. Shafiul Islam and Mr. Yuta Torihata in the experimental work. The discussion with Dr. Matsutaro Seki, BRI has also been greatly acknowledged.

REFERENCES

[1] Alwashali, H., Torihata, Y., Jin, K., & Maeda, M., "Experimental observations on the in-plane behaviour of masonry wall infilled RC frames; focusing on deformation limits and backbone curve," Bull. of Eq. Eng., Vol. 1(25), 2017.

[2] JIS standard, "Method of test for compressive strength of concrete," Japanese Standard Association, 2010.

[3] ASTM Standard, "Standard Test Method for Compressive Strength of Masonry Prisms," ASTM International, West Conshohocken, PA, 2011.

[4] Wight, J. K. and MacGregor, J. G., "Reinforced concrete-Mechanics and Design," Pearson Education Inc., 2009, pp.69-70.

[5] Priestly, M.J.N., Seible, F. and Calvi, G.M., "Seismic Design and Retrofit of Bridges," John Wiley & Sons Inc.,1996, pp. 554-555.

[6] AIJ standard, "AIJ standard for lateral load-carrying capacity calculation of RC structures,", 2010.

[7] ASCE standard, "Seismic rehabilitation of existing building (ASCE/SEI 41-06)" ASCE, Reston, 2007.